A Mixed Combinatorial Optimization Model to Manage the Hydrothermal Dispatch for the Uruguay River Hydroelectric Plant

Claudio Risso[1][0000−0003−0580−3083], Sergio Nesmachnow[1][0000−0002−8146−4012], Rodrigo Porteiro[2][0000−0001−7793−1645], J. Mario Vignolo[1], Emiliano Sierra[2], and Mario Ibarburu[2]

[1] Facultad de Ingeniería, Universidad de la República (UdelaR), Uruguay
{crisso,sergion,jesus}@fing.edu.uy
[2] UTE, Administración Nacional de Usinas y Transmisiones Eléctricas, Uruguay
{rporteiro,esierra,mibarburu}@ute.com.uy

Abstract. This study introduces a Mixed-Integer Optimization Problem (MIP) formulated to manage the hydrothermal dispatch of the Uruguayan electric system, with emphasis on the Salto Grande Hydroelectric Plant on the Uruguay River: a binational project between Argentina and Uruguay that accounts for most of Uruguay's installed hydroelectric capacity. The article supplements a previous work [11], where the non-linear production of the Río Negro Hydroelectric Complex was incorporated into a MIP. That complex is less significant for its generation capacity (power) than for its crucial storage capabilities (energy). The present work complements the earlier study by modeling the other major component of the Uruguayan hydroelectric system. Simulation results, based on historical inflow and demand data, show that the proposed approach can substantially reduce operating costs and enhance system resilience compared with traditional methods.

Keywords: Mixed-Integer Programming, Hydrothermal Dispatch, Binational Hydropower Operations

1 Introduction

Hydrothermal dispatch continues to be a cornerstone of Uruguay's electricity system planning and operation, balancing a highly renewable mix with large storage facilities and thermal backup. A previous contribution [11] introduced a Mixed-Integer Programming (MIP) model tailored to the interdependent reservoirs and operational constraints of the Río Negro Hydroelectric Complex, the country's main energy storage facility. That study demonstrated how enhanced modeling of water values and unserved-energy penalties can improve the reliability and economic efficiency of dispatch decisions. The model in this work replaces the Río Negro Complex with the Salto Grande Hydroelectric Plant. Situated on the Uruguay River, at the border between Argentina and Uruguay, Salto Grande differs from the Río Negro Complex in several key aspects:

i) it is a binational facility with a much larger installed capacity–1890 MW in total, of which the half (945 MW) corresponds to Uruguay, compared to a total of 603 MW at Río Negro;
ii) on average, the Uruguay River provides significantly higher inflows, 4800 $\frac{m^3}{s}$ versus 1060 $\frac{m^3}{s}$ at Río Negro;
iii) however, its natural inflows exhibit much greater variability, fluctuating between 5% and 600% of the mean flow depending on weather conditions, whereas Río Negro has registered a maximum of 300% of its average;
iv) with no new inflows, Salto Grande's reservoir can be depleted in less than a week at full production, while the Río Negro Complex can sustain a large share of its maximum capacity for up to six months.

These characteristics make Salto Grande a critical component of Uruguay's energy system in scenarios of high penetration of intermittent renewables.

The aim of this study is to develop and test an optimization model that reflects the system's unique characteristics. By incorporating binational operational constraints, variable inflows, and the actual penalties from the Uruguayan electricity market for unmet demand, the model offers a more realistic view of operational complexity. Similar to [11], it supports decision-making over a two-week horizon, where linear approximations and static water values are insufficient. The study updates the quantitative assessment of Uruguay's hydro resources in a context of rising renewable penetration. Unlike earlier work focused on the Río Negro cascade, this analysis includes the country's largest hydro plant, embedded in a complex institutional setting. Comparing results with historical operations and with the MIP model for the Río Negro Complex highlights shared challenges and opportunities to enhance system resilience and efficiency.

The remainder of this paper is organized as follows. Section 2 reviews previous work on hydrothermal dispatch, mixed-integer programming approaches, and binational hydroelectric operations. Section 3 describes the Uruguay River Hydroelectric System, providing key technical and operational details of the Salto Grande Plant and its complementarity with the Río Negro Complex. Section 4 then presents the proposed Mixed-Integer Optimization Model, detailing its formulation, decision variables, and constraints. Section 5 outlines the case study setup, including data sources, scenario generation, and instance characteristics. Section 6 reports and discusses the main results, highlighting dispatch patterns, cost reductions, and reliability metrics. Finally, Section 7 concludes the paper and outlines avenues for future research.

2 Related Work

This section reviews the main research underpinning the proposed model, beginning with the foundational work on Stochastic Dynamic Programming (SDP) for hydrothermal dispatch, then addressing the limitations of classical approaches. It concludes by highlighting studies on South American hydro systems and binational operations, which frame the institutional and regional context for the modeling choices in this study.

2.1 Hydrothermal Dispatch via Stochastic Dynamic Programming

Foundational work on Dynamic Programming (DP) and Stochastic Dynamic Programming (SDP) established the theoretical basis for multi-stage decision-making under uncertainty [1, 2]. In the hydrothermal context, SDP has been widely applied to compute medium- and long-term water values, propagate them across cascaded systems, and guide short-term linear dispatch models [4, 6]. Classic examples include large-scale applications in Brazil, Chile, and Colombia [3], where SDP-based approaches underpin national planning. In Uruguay, the SDP-based methodology and its institutional embedding are documented in both technical literature and the national regulatory framework, which formalizes the computation and use of water values for Rincón del Bonete and their downstream propagation to Palmar, as well as for Salto Grande [5, 13]. While effective, SDP suffers from the curse of dimensionality, limiting scalability when additional state variables (e.g., contracts, extended horizons, or high renewable penetration) are introduced.

2.2 Mixed-Integer and Stochastic Programming Advances

To address SDP's scalability limitations, mixed-integer and stochastic programming formulations have been developed to coordinate hydrothermal systems with richer operational constraints and piecewise-linear approximations of nonlinear production functions [7, 12]. Representative formulations capture reservoir and unit-commitment couplings with improved fidelity [10, 8], scenario-based inflows, and reliability penalties. Building on this line, a recent contribution for the Río Negro Hydroelectric Complex introduced a Mixed-Integer Programming (MIP) model that refines unserved-energy penalties and water valuation using piecewise-linear representations, improving cost and reliability metrics in short-term horizons [11]. Comparable approaches have been tested in the Paraná River Basin in Brazil and the Caroní Basin in Venezuela [3], showing that mixed-integer formulations can successfully replicate large hydro systems under uncertainty.

2.3 South American Hydro Systems and Binational Operations

South American power systems feature large hydro shares with heterogeneous storage and inflow regimes, often requiring cross-border coordination. In Uruguay, the coexistence of a domestic cascade (Río Negro) and a binational high-capacity plant (Salto Grande) poses distinct modeling challenges: intertemporal coupling across multiple reservoirs in the former, and high inflow variability with institutional constraints in the latter [5, 13]. Several studies on binational or shared-basin operations highlight the importance of institutional rules in dispatch decisions, such as analyses of the Itaipú Binational Power Plant governance framework [9]. These characteristics motivate optimization frameworks that can simultaneously represent stochastic hydrology, operational rules, and contractual arrangements over horizons beyond day-ahead, while remaining computationally tractable for real-world use.

3 The Uruguay River Hydroelectric System

This section presents an overview of the Uruguay River Hydroelectric System, with emphasis on the Salto Grande Hydroelectric Plant and its interaction with the domestic Río Negro Complex. It first outlines the plant's location, technical features, and institutional framework, then examines its complementarity with the Río Negro Complex, highlighting differences in inflow regimes, storage capacity, and operational constraints. These elements provide the basis for the Mixed-Integer Optimization Model introduced in the next section.

3.1 Salto Grande Plant Overview

The Salto Grande Hydroelectric Plant is located on the Uruguay River at approximately 320 km northwest of Montevideo and 450 km north of Buenos Aires. It constitutes a binational infrastructure jointly owned and operated by Argentina and Uruguay under the framework of the Salto Grande Joint Technical Commission. The plant is equipped with 14 Kaplan-type turbines, with a total installed capacity of 1890 MW, equally divided between Uruguay and Argentina (7 units each). This allocation may be temporarily unbalanced in response to the needs of each country, subject to short-term bilateral agreements.

The reservoir formed by the dam extends over 783 km^2, providing a storage capacity capable of several days of full-power generation under average hydrological conditions. Hydrological data show that the Uruguay River, which feeds Salto Grande, has an average inflow of 4800 $\frac{m^3}{s}$, though with substantial variability. This makes Salto Grande not only the largest but also the most hydrologically volatile source of electricity in Uruguay's system. Moreover, the plant's operation must comply with minimum ecological flows, navigation constraints, and binational energy-sharing agreements, all of which add layers of complexity to dispatch decisions. These conditions are fundamentally different from those of the three-dam cascade on the Río Negro, which is entirely within Uruguayan territory and under a single operator.

The Salto Grande facility plays a strategic role in Uruguay's generation mix, supplying between 15% and 25% of the country's electricity demand depending on hydrological conditions. As with the reservoirs of the Río Negro Complex, the Salto Grande reservoir functions as a short-term buffer for intermittent renewables –particularly wind and solar– by enabling rapid ramping and flexible water storage. As a result, the plant serves both as a large-scale energy provider and as a system stabilizer in the face of renewable variability. The figure *Days to Empty at Full Power* in Table 1 assumes average inflows. Without them, the periods drops to less than a half.

3.2 Complementarity with the Río Negro Complex

Although both the Salto Grande Plant and the Río Negro Hydroelectric Complex are central to Uruguay's hydroelectric system, they differ substantially

Table 1. Technical parameters of the Salto Grande Hydroelectric Plant [source: UTE and Salto Grande Joint Technical Commission].

Parameter	Uruguay Share	Total	Unit	Notes
Number of Turbines	7	14	–	Kaplan-type
Installed Capacity	945	1890	MW	Uruguay / Total
Reservoir Surface	783		km^2	Average level
Average Inflow	4800		m^3/s	Long-term mean
Minimum Ecological Flow	500		m^3/s	Regulatory constraint
Days to Empty at Full Power	15		days	Assuming no inflows

in their structure, mode of operation, and strategic function. The Río Negro Complex comprises three sequential plants –Rincón del Bonete, Baygorria, and Palmar– arranged in a cascade configuration along a river located entirely within Uruguayan territory. This configuration creates strong interdependence among reservoir levels and requires coordinated operation, while also providing the country with its largest long-term energy storage asset: the Bonete reservoir, which can sustain full output for over half a year.

In contrast, Salto Grande is a single large plant with a much larger installed capacity but far less storage relative to inflow and with substantially higher variability. While the Río Negro Complex can be modeled as an integrated system with shared state variables and coordinated dispatch, Salto Grande must be treated as a high-capacity but low-storage facility with binational constraints, separate decision-making processes, and compliance with international treaties. Furthermore, its proximity to the Argentine grid and to major industrial centers in the littoral region makes its dispatch sensitive to cross-border transmission conditions and export/import opportunities.

From an optimization perspective, these differences imply distinct model structures. In the case of the Río Negro Complex, the main challenge is to capture the intertemporal linkages among multiple reservoirs and turbines, whereas for Salto Grande the main challenge is to handle stochastic inflows, large instantaneous capacities, and institutional constraints. The MIP model developed for this study reflects these distinctions by introducing new decision variables, extended constraint sets, and scenario-based inflow representations to adequately capture the operational behavior of the Uruguay River hydroelectric resource.

4 Mixed-Integer Optimization Model

Since the operation of Salto Grande is driven by distinct needs, several considerations must be addressed before delving into the modeling details. A straightforward dichotomic approach distinguishes between two scenarios with respect to the Argentine and Uruguayan energy markets: i) short-term forecasts of wind, solar, and hydrological resources suggest that Uruguay is likely to meet its residual demand over the following two weeks without the need of Salto Grande; ii) the projected availability of resources positions Salto Grande as a critical element for the operation of the Uruguayan system.

The first scenario corresponds to that described in [11], where national requirements are addressed independently of Salto Grande's participation. In this context, binational energy-sharing agreements allow Argentina to operate the plant's full capacity according to its own needs, with the understanding that such energy will later be compensated. Conversely, at some periods, Uruguay may operate the dam as if it were solely under its control, optimizing its dispatch within the framework of its national system planning. This work focuses on a variant of the second scenario, in which Salto Grande's short-term operation plays a key role in the Uruguayan system. In this case, its dispatch is scheduled according to national needs, while accounting for the fact that a portion of the generated energy must supply the Argentine market.

4.1 The Salto Grande Dam

In this section, we examine the subproblem to be integrated into a MIP in order to capture the generation of Salto Grande. The operation of a hydroelectric unit can be described using four technical variables. The control variables $x_{4h,t}$ and $y_{4h,t}$ represent, respectively, the turbinated flow $[\frac{\mathrm{m}^3}{\mathrm{s}}]$ and the spillage $[\frac{\mathrm{m}^3}{\mathrm{s}}]$ at time interval t. The distinction between them lies in the fact that only the flow passing through the turbines produces electricity, represented by the derived variable $g_{4h,t}$, which measures energy generation [MW] during the interval. For units equipped with a dam and reservoir, a state variable $v_{4h,t}$ is also included, representing the reservoir volume [m^3]. The subindex 4 is used for Salto Grande's variables, as subindices 1 to 3 were assigned to Bonete, Baygorria, and Palmar in [11]. In this context, the production function of Salto Grande in (1) resembles that of Palmar, a high-capacity unit with no downstream plants.

$$
\begin{aligned}
P(x_{4h}, y_{4h}, v_{4h}) = \sum_{t=1}^{T} & p_4^{(1)} x_{4h,t} + p_4^{(2)} x_{4h,t} v_{4h,t} - p_4^{(3)} x_{4h,t} v_{4h,t}^2 - p_4^{(4)} x_{4h,t}^2 \\
& - p_4^{(4)} x_{4h,t} y_{4h,t} + p_4^{(5)} x_{4h,t}^3 + p_4^{(5)} x_{4h,t} {y_{4h,t}}^2 + 2 p_4^{(5)} {x_{4h,t}}^2 y_{4h,t},
\end{aligned} \tag{1}
$$

Based on the data provided by UTE, the minimum reference storage volume in the Salto Grande reservoir is 0 hm^3, corresponding to a lake level of 30.1 m. The maximum storage volume is 4017 hm^3, associated with a level of 37 m. The maximum turbine discharge at Salto Grande is 8300 $\frac{\mathrm{m}^3}{\mathrm{s}}$, which, at the maximum level and with zero spillage, corresponds to an output of 1890 MW, as in Table 1. Under these conditions, the time required to fully deplete the reservoir –without new inflows– starting from its maximum level is less than 6 days, i.e., less than half of the reference planning horizon. This evinces that it makes no sense to take non-linear values from long-term planning models. This scenario assumes that the energy in (1) is adjusted according to Uruguayan needs, although it is shared with Argentina at a ratio $0 < r \leq 1$, so Uruguay receives $r \cdot P(x_{4h}, y_{4h}, v_{4h})$.

The reference year for hydrological inflows was set to 2011, the same year used in [11]. Year 2011 was chosen for the Río Negro as it was the driest year in the period reported by UTE. As shown in Figure 1, the hydrological conditions of the Uruguay River in 2011 were far from those of the Río Negro. The total inflows to

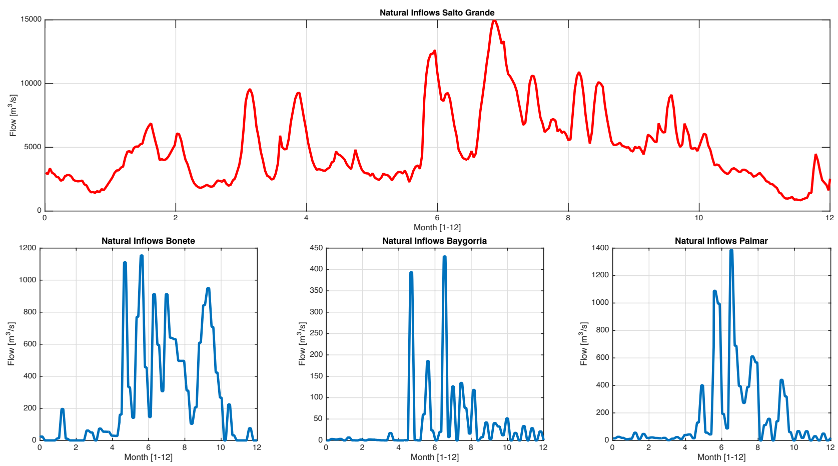

Fig. 1. Hydrological inflows from the Uruguay River to the Salto Grande reservoir [top, red], and inflows to the three reservoirs of the Río Negro [bottom, blue].

the Salto Grande reservoir during 2011 amounted to 156.789 hm^3, equivalent to 39 times the reservoir's maximum storage capacity. Over the same period, inflows to the Río Negro were: Bonete 8835 hm^3, Baygorria 1160 hm^3, and Palmar 5497 hm^3, which together represent only 9.9% of the volume received at Salto Grande. Data validate the second scenario at the beginning of this section, where Salto Grande is important to preserve the Río Negro's resources. As in [11], a reference set of optimized controls was used to simplify (1), where spillage is relatively low, which in this case is approximated by

$$g_{4h,t} = (\hat{p}^{(1)}_{4h} x_{4h} - \hat{p}^{(4)}_{4h} x^2_{4h}) + (\hat{p}^{(2)}_{4h} v_{4h} - \hat{p}^{(3)}_{4h} v^2_{4h}) x_{4h}. \tag{2}$$

The approximation that minimizes the annual mean error between (2) and (1) consists simply of using $\hat{p}^{(k)}_{4h} = 0.99 \cdot p^{(k)}_{4h}$, which keeps the mean error below 1% of the actual value, though the maximum error reaches 68.1 MWh during periods of high spillage in 2011, when y_{4h} approached 5000 $\frac{\mathrm{m}^3}{\mathrm{s}}$. Considering that the average spillage in 2011 was 226.7 $\frac{\mathrm{m}^3}{\mathrm{s}}$, it appears reasonable to set an upper bound of $y_{4h} \leq 3000$ $\frac{\mathrm{m}^3}{\mathrm{s}}$ for optimized management. In this case, using $\hat{p}^{(k)}_{4h} = 0.985 \cdot p^{(k)}_{4h}$ results in a maximum error of 47.9 MWh, an average hourly error of 15.4 MWh, and a mean error in the total energy generated during 2011 of 1.5%. In (2), the leading terms in parentheses –which account for the greatest relative weight– correspond to a concave function, which can be approximated with negligible error by the maximum of a set of four tangents in Figure 2. Since

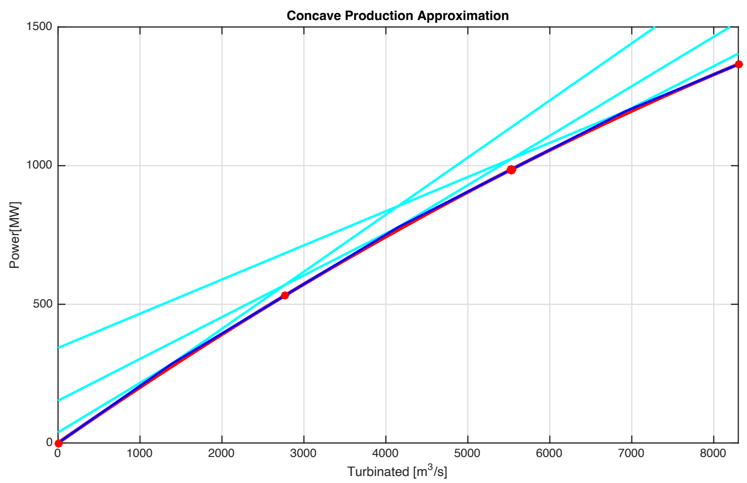

Fig. 2. Actual concave production [red], tangents at the four indicated points [light blue], and the resulting approximation [blue].

energy $g_{4h,t}$ is a scarce resource to be managed within an optimization problem, it is expected to be maximized. Accordingly, the leading term is modeled through the following set of equations:

$$\begin{cases} z_{4h,t} \leq \hat{r}_{4h}^{(1)} x_{4h,t}, & (i) \\ z_{4h,t} \leq \hat{r}_{4h}^{(2)} x_{4h,t} + \hat{s}_{4h}^{(2)}, & (ii) \\ z_{4h,t} \leq \hat{r}_{4h}^{(3)} x_{4h,t} + \hat{s}_{4h}^{(3)} & (iii) \\ z_{4h,t} \leq \hat{r}_{4h}^{(4)} x_{4h,t} + \hat{s}_{4h}^{(4)} & (iv) \end{cases}, \tag{3}$$

for certain constants $\hat{r}_{4h}^{(i)}$ and $\hat{s}_{4h}^{(i)}$. The second term in (2) captures the additional output resulting from an increased reservoir head, which is likewise expected to be maximized. To represent this effect, the reservoir level is discretized into six intervals using five thresholds: $\overline{V4h_1}$ to $\overline{V4h_5}$, and two types of auxiliary variables are introduced. In particular, five continuous artificial variables, $\theta_{4h,t}^{(i)}$ $(1 \leq i \leq 5)$, are used to approximate the additional production associated with the head. To assemble a production proxy we introduce (4).

$$g_{4h,t} = z_{4h,t} + \sum_{i=1}^{5} \theta_{4h,t}^{(i)}. \tag{4}$$

To maintain consistency, the optimization is allowed to activate the surplus of $\theta_{4h,t}^{(i)}$ only when the reservoir volume permits. To this end, boolean variables

$\varphi^{(i)}_{4h,t}$ $(1 \leq i \leq 4)$ and equations (5), (6) are introduced. Equation (5) sets upper bounds for $\theta^{(i)}_{4h,t}$, which can be made proportional to the turbine discharge $x_{4h,t}$, provided that the variables $\varphi^{(i)}_{4h,t}$ allow it.

$$\begin{cases} 0 \leq \theta^{(1)}_{4h,t} \leq (\hat{p}^{(2)}_{4h}\overline{V4h_1} - \hat{p}^{(3)}_{4h}\overline{V4h_1}^2)x_{4h,t}, & (i) \\ 0 \leq \theta^{(2)}_{4h,t} \leq (\hat{p}^{(2)}_{4h}\Delta\overline{V4h_2} - \hat{p}^{(3)}_{4h}\Delta\overline{V4h_2}^2)x_{4h,t}, & (ii) \\ 0 \leq \theta^{(2)}_{4h,t} \leq 8300(\hat{p}^{(2)}_{4h}\Delta\overline{V4h_2} - \hat{p}^{(3)}_{4h}\Delta\overline{V4h_2}^2)\varphi^{(1)}_{4h,t}, & (iii) \\ 0 \leq \theta^{(3)}_{4h,t} \leq (\hat{p}^{(2)}_{4h}\Delta\overline{V4h_3} - \hat{p}^{(3)}_{4h}\Delta\overline{V4h_3}^2)x_{4h,t}, & (iv) \\ 0 \leq \theta^{(3)}_{4h,t} \leq 8300(\hat{p}^{(2)}_{4h}\Delta\overline{V4h_3} - \hat{p}^{(3)}_{4h}\Delta\overline{V4h_3}^2)\varphi^{(2)}_{4h,t} & (v) \\ 0 \leq \theta^{(4)}_{4h,t} \leq (\hat{p}^{(2)}_{4h}\Delta\overline{V4h_4} - \hat{p}^{(3)}_{4h}\Delta\overline{V4h_4}^2)x_{4h,t}, & (vi) \\ 0 \leq \theta^{(4)}_{4h,t} \leq 8300(\hat{p}^{(2)}_{4h}\Delta\overline{V4h_4} - \hat{p}^{(3)}_{4h}\Delta\overline{V4h_4}^2)\varphi^{(3)}_{4h,t} & (vii) \\ 0 \leq \theta^{(5)}_{4h,t} \leq (\hat{p}^{(2)}_{4h}\Delta\overline{V4h_5} - \hat{p}^{(3)}_{4h}\Delta\overline{V4h_5}^2)x_{4h,t}, & (viii) \\ 0 \leq \theta^{(5)}_{4h,t} \leq 8300(\hat{p}^{(2)}_{4h}\Delta\overline{V4h_5} - \hat{p}^{(3)}_{4h}\Delta\overline{V4h_5}^2)\varphi^{(4)}_{4h,t} & (ix) \end{cases} \tag{5}$$

These variables, in turn, are sequentially activated in (6) according to the reservoir state $v_{4h,t}$, what binds state and control variables. Parameters $\overline{V4h_1}$ to $\overline{V4h_5}$ and $M4$ were calibrated based on a series of optimized solutions and are defined relative to the initial water stock in the Salto Grande reservoir, while the others are computed as $\Delta\overline{V4h_j} = \overline{V4h_j} - \overline{V4h_{j-1}}$ and $\Delta\overline{V4h_j}^2 = (\overline{V4h_j} - \overline{V4h_{j-1}})^2$.

$$\begin{cases} \varphi^{(1)}_{4h,t} \leq 1 - (\overline{V4h_2} - v_{4h,t})/M4, \\ \varphi^{(2)}_{4h,t} \leq 1 - (\overline{V4h_3} - v_{4h,t})/M4, \\ \varphi^{(3)}_{4h,t} \leq 1 - (\overline{V4h_4} - v_{4h,t})/M4, \\ \varphi^{(4)}_{4h,t} \leq 1 - (\overline{V4h_5} - v_{4h,t})/M4 \end{cases} \tag{6}$$

To track the reservoir volume, the model includes equations representing the water balance in m^3, at each one hour (3600 seconds) interval:

$$v_{4h,t} = v_{4h,t-1} + 3600(a_{4h,t} - x_{4h,t} - y_{4h,t}), \tag{7}$$

where $a_{4h,t}$ denotes the natural inflows from the Uruguay River into the reservoir. To conclude the modeling of Salto Grande, it is necessary to define a cost associated with its use. Energy generation results from converting natural inflows into electricity, which incurs no direct cost. Moreover, as noted, the entire reservoir can be depleted within the planning horizon $T = 15$ days. Consequently, the valuation of water resources is indirect and arises from longer-term considerations, such as: low end-of-period water levels reducing efficiency in subsequent planning stages due to lower head; excessive use of Salto Grande's production for Uruguay potentially limiting future allocations in favor of Argentina; and the possible resulting overuse of water at the Río Negro Complex, which has much longer storage capability. This long-term valuation is beyond the scope of the present work. Here, we simply assume a linear cost associated with the balance of the reservoir volume over the planning period: $ca_{4h}(v_{4h,0} - v_{4h,T})$.

4.2 A Simple Thermal Power Unit

To extend the model, we include a 200 MW thermal unit (`T1`) with a variable cost of $ct_1 = 100$ USD/MWh. Its integration is simpler than the hydropower equations in Section 4.1, requiring only one control variable, $0 \leq g_{1t,t} \leq 200$, for thermal generation at time t. Total output becomes $g_t = r \cdot g_{4h,t} + g_{1t,t}$, with operating costs directly tied to fuel use $ct_1 \sum_{t=1}^{T} g_{1t,t}$.

4.3 Failure Costs

The regulation for the Uruguayan electric market establishes fines for not fulfilling the entire demand of the system, which are referred to as *failure cost*. These fines are specified in the Electricity Market Regulations and listed in Table 2. The penalty is defined for the percentages of unmet demand, in an incremental manner. Thus, if at a given hour t the demand were $d_t = 1000$ MWh, and only 900 MWh were dispatched, the total shortfall would be 100 MWh, and the penalty applied for that hour would amount to 109.400 USD. Broke down costs are provided in Table 3. Regarding the failure cost model, which in model [11]

Table 2. Incremental failure costs established in the Electricity Market Regulations, according to the percentage of hourly demand (d_t) affected.

Demand Step (% d_t)	**0% a 2%**	**2% a 7%**	**7% a 14.5%**	**14.5% a 100%**
Failure Cost [USD/MWh]	370	600	2400	4000

Table 3. Example of how to apply failure costs in an hour with a total demand of 1000 MWh and a shortfall of 100 MWh.

Failure Level	**min [MWh]**	**max [MWh]**	**Cost [USD/MWh]**	**Shortfall [MWh] per Step**	**Subtotal [USD] per Step**
Step 1	0	20	370	20	7400
Step 2	20	70	600	50	30000
Step 3	70	145	2400	30	72000
Step 4	145	1000	4000	0	0
Total				100	109400

included a cost-term $CF \sum_{t=1}^{T}(d_t - g_t)$, in this new version it is replaced by:

$$\begin{cases} CFT = \sum_{t=1}^{T} f_t \\ f_t \geq \max\{0, \hat{q}_{1f}^{(1)}(d_t - g_t)\} \quad (i) \\ f_t \geq \hat{p}_{1f}^{(2)} + \hat{q}_{1f}^{(2)}(d_t - g_t) \quad (ii) \\ f_t \geq \hat{p}_{1f}^{(3)} + \hat{q}_{1f}^{(3)}(d_t - g_t) \quad (iii) \\ f_t \geq \hat{p}_{1f}^{(4)} + \hat{q}_{1f}^{(4)}(d_t - g_t) \quad (iv) \end{cases} \tag{8}$$

The CFT from (8) goes into the objective function of the problem. The rest are constraints. The parameters $\hat{q}_{1f}^{(i)}$ are the penalties [USD/MWh] established in the regulations (see Table 2). The $\hat{p}_{1f}^{(i)}$ are set to ensure continuity between one step and the next. It is worth noting that this relatively simple formulation is made possible by the regulatory framework, which establishes fines with progressive costs or slopes, resulting in a convex subproblem for a cost to be minimized within the larger optimization problem. However, since this extended failure cost model is parameterized by the energy demand d_t at each interval ($1 \leq t \leq T$), it requires the introduction of as many f_t variables as there are intervals (360), unlike the formulation in [11]. Finally, that work used penalty values of 1600 USD/MWh and 3200 USD/MWh for failures, which, according to Table 3, approximately correspond to step 3, confirming that that choice was aligned with actual data.

5 Case Study Setup

The Uruguayan power system, whose energy mix includes very high shares of solar and especially wind generation, does not rely on batteries to shape the output of these uncontrollable sources. Instead, it achieves control indirectly by managing hydropower to offset the short-term variability of non-conventional renewable energies. This is done by dispatching the so-called *residual demand*: the difference between actual demand and the generation supplied by wind and solar power. The test instances in this work were constructed from real-world data, following the approach in [11]. In that study, natural inflows and initial reservoir volumes for the Río Negro system were taken from 2011, the driest year within a decade. Residual demand, however, was sourced from 2018, since wind and solar generation in Uruguay were not yet available in 2011; only 40% of that demand was considered, reflecting the approximate share of the Río Negro Complex in the system's capacity.

Although, as shown in Figure 1, the hydrological conditions of the Uruguay River in 2011 differed significantly from those of the Río Negro, as a baseline, we chose to use Salto Grande's inflow records for that year, combined with the residual demand from 2018. In this case, however, 60% of the total residual demand was considered, since Salto Grande's capacity is roughly 50% greater than that of the Río Negro Complex. Another difference between both works lies in the computation of failure costs. National regulations establish penalty levels as a stepped function of the total system demand, as detailed in Table 2. Consequently, both demand measures must be considered in the formulation (8): d_t represents the total system demand at time t used to calculate the failure cost parameters $\hat{p}_{1f}^{(i)}$, while the residual demand $\bar{d}_t$ is used to account for the actual shortfall. For consistency, we used the 60% ratio for both, the total (d_t) and the residual ($\bar{d}_t$) demand. Table 4 summarizes the main characteristics of the 68 instances addressed in this work. The table is organized into three groups of columns: the first two provide instance-specific data, while the third group reports additional information that is common to both instances in each row.

Table 4. Summary of the main attributes of the 68 instances solved.

InstId	ca4h [USD/hm^3]	Residual [MWh]		InstId	ca4h [USD/hm^3]	Residual [MWh]		v4h0 [hm^3]	Inflows [hm^3]	Total Demand
		Total	Relative			Total	Relative			
1	893	151,469	52.6%	**35**	1908	245,209	85.2%	2625.5	3,485	287,749
2	1054	164,674	57.9%	**36**	2298	265,020	93.1%	2256.1	2,400	284,548
3	1109	165,657	57.1%	**37**	2630	266,452	91.8%	945.8	5,503	290,243
4	1841	158,597	56.4%	**38**	3230	255,875	91.0%	2200.5	6,690	281,068
5	3012	152,969	57.1%	**39**	4172	247,450	92.4%	1681.4	4,159	267,887
6	6866	129,114	50.9%	**40**	10011	211,651	83.5%	2509.1	5,059	253,608
7	0	156,211	55.5%	**41**	2545	252,304	89.6%	2133.9	4,813	281,504
8	536	154,787	49.2%	**42**	6783	250,160	79.5%	2250.7	3,571	314,599
9	0	193,568	61.4%	**43**	7168	308,336	97.8%	2688.8	7,858	315,265
10	0	165,797	51.9%	**44**	3350	266,700	83.4%	1807.5	12,121	319,734
11	0	127,900	49.4%	**45**	0	209,839	81.1%	2618.3	6,873	258,683
12	0	121,852	49.8%	**46**	124	200,796	82.0%	2001.5	8,525	244,724
13	63	110,083	44.3%	**47**	144	183,121	73.7%	2719.2	5,886	248,305
14	102	101,099	39.1%	**48**	209	169,628	65.6%	2108.6	3,976	258,693
15	191	114,049	44.9%	**49**	511	189,082	74.5%	2309.3	2,515	253,843
16	296	144,323	55.8%	**50**	867	234,466	90.6%	2104.2	2,310	258,832
17	782	77,436	26.9%	**51**	925	134,164	46.6%	2625.5	3,485	287,749
18	1209	108,928	38.3%	**52**	2103	181,384	63.7%	2256.1	2,400	284,548
19	527	98,561	34.0%	**53**	2114	165,825	57.1%	945.8	5,503	290,243
20	446	103,823	36.9%	**54**	834	173,721	61.8%	2200.5	6,690	281,068
21	1251	104,237	38.9%	**55**	2630	174,353	65.1%	1681.4	4,159	267,887
22	1192	84,109	34.4%	**56**	1940	144,162	59.0%	1731.2	3,129	244,180
23	384	104,490	40.8%	**57**	1187	174,735	68.3%	1115.4	7,534	255,871
24	543	112,768	43.4%	**58**	1162	187,142	72.0%	1696.9	8,183	259,982
25	0	78,421	30.9%	**59**	623	135,621	53.5%	2509.1	5,059	253,608
26	0	119,848	42.6%	**60**	3710	197,743	70.2%	2133.9	4,813	281,504
27	1700	158,424	50.4%	**61**	2750	255,643	81.3%	2250.7	3,571	314,599
28	127	183,965	72.0%	**62**	867	255,511	100.0%	2032.5	8,774	255,511
29	0	162,860	63.0%	**63**	867	258,683	100.0%	2618.3	6,873	258,683
30	173	216,447	88.4%	**64**	419	244,724	100.0%	2001.5	8,525	244,724
31	282	178,065	71.7%	**65**	397	248,305	100.0%	2719.2	5,886	248,305
32	332	112,450	43.5%	**66**	607	186,680	72.2%	2108.6	3,976	258,693
33	327	72,274	28.5%	**67**	425	126,392	49.8%	2309.3	2,515	253,843
34	760	83,427	32.2%	**68**	997	143,147	55.3%	2104.2	2,310	258,832

The first and fifth columns contain the instance indices. The second and sixth columns report the values of ca_{4h} [USD/hm^3], which serve as reference costs for water usage through the term $ca_{4h}(v_{4h,0} - v_{4h,T})$. These values are provided by long-term planning systems. The third and seventh columns present the cumulative residual demand for each instance, $\sum_{t=1}^{T} \bar{d}_t$, while the fourth and eighth columns show this residual demand as a percentage of the total cumulative demand, $\sum_{t=1}^{T} d_t$, which is listed in the last column. Finally, columns nine and ten respectively indicate the initial reservoir volume $v_{4h,0}$ [hm^3] at Salto Grande and the total natural inflows $\sum_{t=1}^{T} a_{4h,t}$ [hm^3] over the planning horizon.

Instances 1 to 34 (Group 1), along with the total demand and hydrological records for Salto Grande, are entirely based on historical data. Along some clear and windy days, the combined residual demand can drop to as little as one quarter of the total demand, it can even get close to zero at some hours. Consequently, in Group 2, residual demands are artificially increased to stress-test the model. This adjustment creates a context that, in longer-term planning, raises the opportunity cost of water at Salto Grande (i.e., ca_{4h} values).

6 Experimental Results and Discussion

Although data differ amid instances in Table 4, all their MIP formulations have the same dimensions, comprising 6120 variables –1440 of which are integer– and 10,080 constraints: 1080 equalities and 9000 inequalities. Instances were solved

Table 5. Summary of the main results for the 68 solutions.

InstId	Salto Grande		Thermal		InstId	Salto Grande		Thermal		Failure	
	[MWh]	[USD]	[MWh]	[USD]		[MWh]	[USD]	[MWh]	[USD]	[MWh]	[USD]
1	151,240	1,332,000	229	22,900	**35**	181,130	5,009,000	60,398	6,039,800	3,679	723,000
2	140,670	2,378,000	24,004	2,400,400	**36**	137,810	5,185,000	71,700	7,170,000	55,499	12,333,000
3	155,290	284,000	10,367	1,036,600	**37**	163,850	1,788,000	62,594	6,259,400	40,043	8,024,000
4	158,600	(2,829,000)	0	0	**38**	183,540	(1,833,000)	69,740	6,974,000	2,612	374,000
5	95,380	(3,235,000)	57,589	5,758,800	**39**	163,300	7,015,000	71,124	7,112,400	13,031	934,000
6	115,150	(10,353,000)	13,966	1,396,500	**40**	139,460	(5,503,000)	69,089	6,908,900	3,123	179,000
7	155,490	0	721	72,100	**41**	191,160	5,011,000	49,042	4,904,100	12,118	2,687,000
8	154,080	903,000	708	70,800	**42**	166,670	15,266,000	70,383	7,038,300	13,124	2,820,000
9	192,200	0	1,372	137,200	**43**	212,420	(3,835,000)	71,541	7,154,100	24,392	4,253,000
10	163,420	0	2,382	238,200	**44**	227,000	(7,402,000)	23,412	2,341,200	16,281	4,204,000
11	127,900	0	0	0	**45**	203,440	0	6,046	604,600	364	39,000
12	121,850	0	0	0	**46**	197,440	(217,000)	3,333	333,300	0	0
13	110,080	(82,000)	0	0	**47**	182,840	12,000	283	28,300	0	0
14	101,100	(78,000)	0	0	**48**	167,440	392,000	2,093	209,300	119	6,000
15	114,050	229,000	0	0	**49**	144,460	1,180,000	44,057	4,405,600	558	57,000
16	129,370	590,000	14,955	1,495,500	**50**	130,390	1,824,000	68,246	6,824,600	35,846	7,380,000
17	77,440	(917,000)	0	0	**51**	134,150	783,000	0	0	0	0
18	108,930	1,351,000	0	0	**52**	140,660	4,745,000	40,735	4,073,500	0	0
19	98,560	(1,101,000)	0	0	**53**	158,660	655,000	7,181	718,000	0	0
20	103,820	(810,000)	0	0	**54**	173,730	(872,000)	0	0	0	0
21	104,240	(960,000)	0	0	**55**	149,780	2,375,000	24,578	2,457,700	0	0
22	84,110	(461,000)	0	0	**56**	142,050	3,358,000	2,113	211,300	0	0
23	104,490	(1,114,000)	0	0	**57**	174,730	(1,492,000)	1	100	0	0
24	112,770	(1,260,000)	0	0	**58**	187,150	(2,004,000)	0	0	0	0
25	78,420	0	0	0	**59**	135,630	(485,000)	0	0	0	0
26	119,850	0	0	0	**60**	127,940	(2,426,000)	69,832	6,983,200	0	0
27	158,420	2,943,000	0	0	**61**	171,520	6,189,000	72,000	7,200,000	12,119	582,000
28	183,970	(252,000)	0	0	**62**	276,280	1,061,000	17,056	1,705,600	615	36,000
29	162,860	0	0	0	**63**	252,770	1,731,000	9,501	950,000	16	1,000
30	216,450	(195,000)	0	0	**64**	280,960	839,000	54,769	5,476,800	6,946	698,000
31	178,070	(50,000)	0	0	**65**	249,770	1,080,000	34,838	3,483,800	492	41,000
32	112,450	(99,000)	0	0	**66**	176,410	1,280,000	10,265	1,026,500	0	0
33	72,270	(105,000)	0	0	**67**	126,410	684,000	0	0	0	0
34	83,430	300,000	0	0	**68**	126,340	1,890,000	16,797	1,679,700	0	0

by means of the software `IBM(R) ILOG(R) CPLEX(R) Interactive Optimizer 22.1.1.0`, running on an server with a `AMD Ryzen 9` processor `7950X3D`, providing 32 cores at 3.0GHz and 32GB of RAM. The optimal solution was found for each instance, using a share $r = \frac{1}{2}$ between Argentina and Uruguay. Computation times were around 1 second for 50 of the 68 instances, and in all cases was obtained within 20 seconds. A summary of the main results for each optimal solution is presented in Table 5, where solution indices match those in Table 4. The columns following *InstId* report the total energy production at Salto Grande and its associated cost, with analogous figures provided for the thermal unit. Failures are absent across all instances in Group 1 (1–34), so no corresponding data are shown. In contrast, frequent failures occur in Group 2, as expected; therefore, two additional columns are included, reporting the total unmet demand and the corresponding penalty, as defined in Table 2.

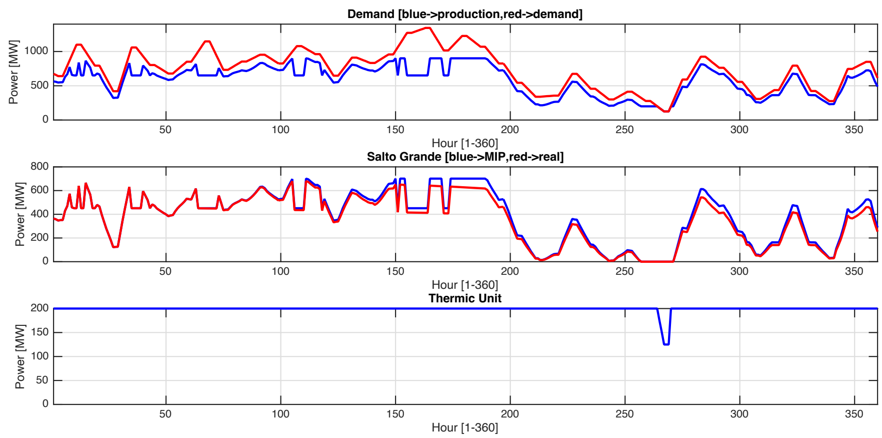

Fig. 3. Hourly profile for Residual Demand ($\bar{d}_t$) and Production of Energy (g_t) [top], Salto Grande MIP model ($g_{4h,t}/2$) and actual production $P(x_{4h}, y_{4h}, v_{4h})$ as in (1) [middle] and Thermal Production ($g_{1t,t}$) [bottom].

Figure 3 presents the hourly profile for instance 36, selected both for its high failure penalty and for exhibiting one of the largest deviations between the MIP approximation ($r \cdot g_{4h,t}$) and the actual production $r \cdot P(x_{4h}, y_{4h}, v_{4h})$. Even so, the similarity between (1) and the solutions obtained by jointly applying (3), (4), (5), and (6) is striking.

7 Conclusions and Future Work

This paper presented a Mixed-Integer Optimization Model (MIP) designed to manage the hydrothermal dispatch of the Uruguayan power system, focusing on the binational Salto Grande Hydroelectric Plant on the Uruguay River. Building upon previous work for the Río Negro Hydroelectric Complex, the proposed model incorporates the distinctive operational characteristics of Salto Grande, including its high installed capacity, limited storage relative to inflows. By explicitly representing piecewise-linear production functions, stepped failure costs, and scenario-based inflows, the model provides a more realistic and tractable formulation for short-term planning horizons. The case study demonstrated the feasibility of solving 68 test instances derived from historical data, offering a detailed quantitative view of how Salto Grande complements the domestic cascade and buffers renewable variability. Together, these results show that mixed-integer formulations can effectively extend classical SDP-based approaches to more complex hydroelectric systems, yielding improved dispatch fidelity and enhanced decision support for Uruguay's renewable-dominated grid.

Future work will extend this model along several directions. First, the integration of longer-term water valuation mechanisms and multi-stage stochastic formulations will allow consistent coordination between short-term dispatch and seasonal storage strategies. Second, testing the model under climate-change-driven inflow scenarios and incorporating probabilistic demand forecasts will improve its robustness under extreme conditions. Finally, implementing the model in a production environment at UTE and coupling it with actual used decision tools will facilitate its adoption as a real-world decision support system for Uruguay's evolving electric grid.

References

1. Bellman, R.: Dynamic Programming. Princeton University Press (1957)
2. Bellman, R.: Dynamic programming in stochastic control. Mathematics of Control (1966)
3. Castellano, A., Martínez, C., Monzón, P., Bazerque, J., et al.: Quadratic approximate dynamic programming for scheduling water resources: a case study in uruguay. arXiv preprint **arXiv:2010.02122** (2020), https://arxiv.org/abs/2010.02122
4. Diniz, A.A.: Short-term hydrothermal coordination model. IEEE Transactions on Power Systems (2014)
5. Ferreira, A.: Uruguayan electricity market regulation and planning. Technical Report (2008)
6. Ferrero, R.: Dynamic valuation of hydroelectric resources. Energy Economics (1998)
7. Hernández, K., Barrera-Singaña, C., Tipán, L.: Hydrothermal economic dispatch incorporating the valve point effect in thermal units solved by heuristic techniques. Energies **18**(11), 2789 (2025). https://doi.org/10.3390/en18112789
8. Martínez, M., et al.: A milp model for generation maintenance scheduling coordinated with hydrothermal dispatch. In: IEEE International Conference on Environment and Electrical Engineering (EEEIC). pp. 1–6 (2020). https://doi.org/10.1109/EEEIC/ICPSEurope49358.2020.9160827
9. Ortigoza, E., Oxilia, V., et al.: Lessons from the itaipu binational power plant in south america: A negotiation framework for transboundary hydropower governance. Water **17**(13), 1947 (2025). https://doi.org/10.3390/w17131947
10. Risso, C.: Mixed-integer formulation for medium-term hydrothermal coordination. Energy Systems (2019)
11. Risso, C., Nesmachnow, S., Porteiro, R., et al.: An enriched mixed combinatorial optimization model to manage the hydrothermal dispatch for the río negro hydroelectric complex. Journal/Conference Name (2024)
12. Santos, R., Diniz, A., Borba, B.: Assessment of the modeling of demand response as a dispatchable resource in day-ahead hydrothermal scheduling – brazil. Energies **15**(11), 3928 (2022). https://doi.org/10.3390/en15113928
13. de la República Oriental del Uruguay, P.: Reglamento del mercado eléctrico uruguayo (2002)